Tight-binding simulation of graphene nanoantenna based on Boltzmann equation and finite difference time-domain method

Shota Ogisawa and Satofumi Souma†
Department of Electrical and Electronic Engineering, Kobe University, Kobe 657-8501, Japan
†email: ssouma@harbor.kobe-u.ac.jp

***Abstract*—We focus on developing a simulation framework for a graphene-based antenna using finite difference time-domain (FDTD) method. Based on the FDTD framework, we consider the propagation of electromagnetic waves in the 2-D space including graphene plane, where the complex graphene conductivity model is employed to take into account the presence of graphene nanoantenna region. In deriving the graphene surface conductivity, we consider the band structure of graphene starting from the atomistic tight-binding model, where the conduction and valence bands meet each other at the K point. In the vicinity of this point, called Dirac point, the dispersion relation is almost linear. Based on such linear dispersion relation near the Dirac point, we calculate the complex graphene surface conductivity in frequency domain based on Boltzmann equation, which can be utilized directly within the FDTD framework. The proposed simulation framework has been successfully worked and we calculated the current density on the surface of graphene nanoantenna.**

I. Introduction

Since the discovery of isolated and stable graphene films in 2004 [1], graphene has attracted intense attention of the entire research community [2] due to its extraordinary mechanical, electronic, and optical properties, which include sufficient electrical conductivity, high optical transmittance, elevated Young's modulus, and thermal conductivity, among others [3], [4], [5], [6], [7]. As researchers investigate the possibilities of the applications of graphene materials, ranging from field-effect transistors to waveguides, electrodes and THz patch antenna [8], [9], [10], [11], the need for an electromagnetic simulation tool for graphene-based devices emerges.

Simulating graphene-based devices in time domain has several advantages. The transient behavior of the device can be observed and the result for a wide frequency band can be obtained from a single simulation in time domain. However, the complicated graphene conductivity model and the electronic/quantum transport occurring in graphene make modeling of graphene challenging. This is especially true for time domain simulations because the graphene conductivity is frequency dependent. As such, the development of an accurate and efficient time domain simulation tool for graphene is important to further study graphene-based devices.

With this motivation, we propose a simulation framework for a graphene-based antenna using finite difference time-domain (FDTD) method. FDTD method is a rigorous and powerful tool for modeling nano-scale devices such as nanoantennas. Based on FDTD framework, we simulate the propagation of electromagnetic waves in the 2-D simulation space including graphene plane, where the complex graphene conductivity model is employed to take into account the presence of graphene nanoantenna region. When modeling a graphene nanoantenna, we calculate the complex graphene surface conductivity (in unit of [S]) based on Boltzmann equation, which can be utilized directly within the FDTD framework.

II. Model and method

The finite-difference time-domain (FDTD) method is a numerical method to solve the time-dependent Maxwell's equations (in partial differential form) based on Yee's work in 1966 [12]. Faraday's Law and Ampere's Law are discretized using central-difference approximations to update the electric fields E and magnetic fields H in space and time. In [12], the Yee's cell of dimension $\Delta x \times \Delta y \times \Delta z$ is introduced as a unit cell of the discretized spatial domain as shown in Fig. 1. The E fields and H fields are defined in an interlinked way such that each E nodes are surrounded by 4 H nodes and vice versa, and the E nodes and H nodes are dislocated by half a cell spatially. All fields are initially set to zero in the simulation domain. With a source of excitation, all E fields are updated at the integer time step n, and H fields are updated at half time step $n + \frac{1}{2}$ using the E values at time step n. Repeating this process allows the simulation to march in time.

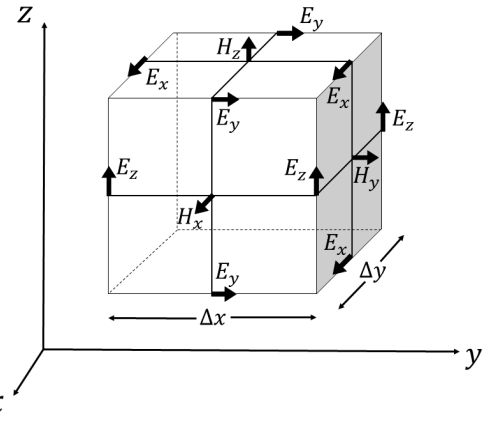

Fig. 1. Yee's cell with E and H fields positions in the unit cell. The E fields and H fields are defined in an interlinked way such that each E nodes are surrounded by 4 H nodes and vice versa, and the E nodes and H nodes are dislocated by half a cell spatially.

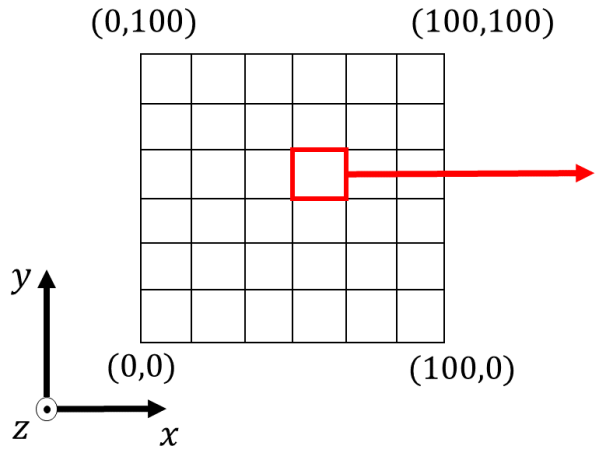

Fig. 2. The 2-D simulation domain has been discretized into 100 × 100 lattice points in the xy plane.

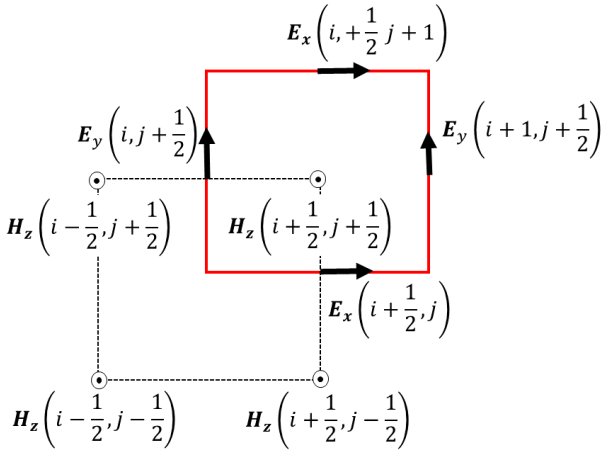

Fig. 3. The arrangement of E_x, E_y and H_z nodes in the 2-D unit cell in the TE mode. Each H nodes are surrounded by four E nodes, while E nodes are located at the center of the two adjacent H nodes.

When simulating a transverse electric (TE) wave propagation, the 2-D simulation domain has been discretized into 100 × 100 lattice points in the xy plane as Fig. 2 shows. In the TE mode, the electric field is transverse to the direction of propagation while the magnetic field is normal to the direction of propagation. Based on FDTD method, electric components E_x, E_y and magnetic component H_z are calculated in the xy-plane as

$$E_x^n\left(i+\frac{1}{2},j\right)=C_{EX}\left(i+\frac{1}{2},j\right)E_x^{n-1}\left(i+\frac{1}{2},j\right)+C_{EXLY}\left(i+\frac{1}{2},j\right)\left\{H_z^{n-\frac{1}{2}}\left(i+\frac{1}{2},j+\frac{1}{2}\right)-H_z^{n-\frac{1}{2}}\left(i+\frac{1}{2},j-\frac{1}{2}\right)\right\} \tag{1}$$

$$E_y^n\left(i,j+\frac{1}{2}\right)=C_{EY}\left(i,j+\frac{1}{2}\right)E_y^{n-1}\left(i,j+\frac{1}{2}\right)-C_{EYLX}\left(i,j+\frac{1}{2}\right)\left\{H_z^{n-\frac{1}{2}}\left(i+\frac{1}{2},j+\frac{1}{2}\right)-H_z^{n-\frac{1}{2}}\left(i-\frac{1}{2},j+\frac{1}{2}\right)\right\} \tag{2}$$

$$\begin{aligned}H_z^{n+\frac{1}{2}}\left(i+\frac{1}{2},j+\frac{1}{2}\right)&=H_z^{n-\frac{1}{2}}\left(i+\frac{1}{2},j+\frac{1}{2}\right)\\&-C_{HZLX}\left(i+\frac{1}{2},j+\frac{1}{2}\right)\left\{E_y^n\left(i+1,j+\frac{1}{2}\right)-E_y^n\left(i,j+\frac{1}{2}\right)\right\}\\&+C_{HZLY}\left(i+\frac{1}{2},j+\frac{1}{2}\right)\left\{E_x^n\left(i+\frac{1}{2},j+1\right)-E_x^n\left(i+\frac{1}{2},j\right)\right\}.\end{aligned} \tag{3}$$

Here the constant C can be calculated by using the permittivity ϵ and permeability μ of a medium, the spatial mesh Δx and Δy, and the value of timestep Δt. We can determine the value of timestep Δt from the following Courant condition

$$c\Delta t \le \frac{1}{\sqrt{\left(\frac{1}{\Delta x}\right)^2+\left(\frac{1}{\Delta y}\right)^2}}, \tag{4}$$

where c is the speed of light.

In deriving the graphene surface conductivity, we consider the band structure of graphene starting from the atomistic tight-binding model. Atomistic tight-binding model is an approach to the calculation of electronic band structure using an approximate set of wave functions based upon superposition of wave functions for isolated atoms located at each atomic site. As shown in Fig. 4 (right), in derived band structure of graphene, the conduction and valence bands meet each other at K point, which is like a zero band gap semiconductor [13]. The six points in the two dimensional Brillouin zone where the bands meet are called Dirac points. In the vicinity of these points, the dispersion relation is almost linear and described as $\epsilon(k) = \pm\hbar v_F k$, where $\hbar$ is the reduced Planck's constant, v_{F} is the Fermi velocity, and k is the wavenumber in m^{-1}.

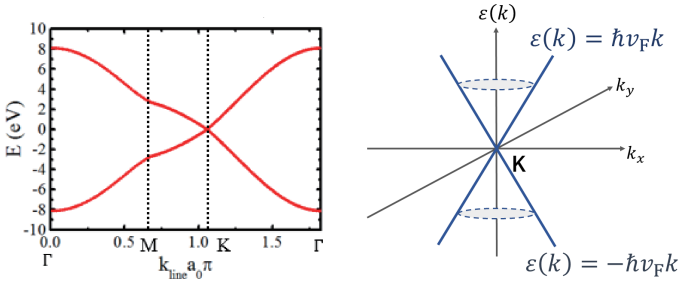

Fig. 4. (left) Energy band structure of graphene. The conduction and valence bands meet each other at K point. (right) In the vicinity of K point, the dispersion relation is almost linear, where $\epsilon(k) = \pm\hbar v_F k$.

Based on such linear dispersion relation near the Dirac point and by restricting our focus only on the intraband contribution (thus neglecting interband contribution), we calculate the complex graphene surface conductivity in frequency domain based on Boltzmann equation. The Boltzmann equation describes the statistical behavior of a thermodynamic system not in a state of equilibrium. In following equation, E_{F} is the Fermi energy. ω is the angular frequency in radians and τ_{scat} is the scattering rate in seconds. Also, T is the temperature in Kelvin, $-e$ is the electron charge, $\hbar$ is the reduced Planck's constant, and k_{B} is the Boltzmann constant. In the case of homogeneous systems, the distribution function $f_j(\mathbf{k}, t)$ for the jth band ($j = 1$ and $j = 2$ are valence and conduction band, respectively)

is determined by the Boltzmann equation

$$\frac{\partial f_j(\mathbf{k},t)}{\partial t} = \frac{\partial f_j(\mathbf{k},t)}{\partial k_x}\left(-\frac{qE}{\hbar}\right) + P_j(\mathbf{k}), \tag{1}$$

where the scattering term $P_j(\mathbf{k})$ is given within the relaxation time approximation as

$$P_j(\mathbf{k}) = -\frac{f_j(\mathbf{k},t) - f_j^{(\mathrm{eq})}(\mathbf{k},t)}{\tau_{\mathrm{scat}}}. \tag{2}$$

Here we have assumed that the electric field along the x direction. By making use of the dispersion relation of graphene $\varepsilon_j(\mathbf{k}) = \hbar v_{\mathrm{F}}\sqrt{k_x^2+k_y^2}$, k_x derivative of the distribution function $f_j(\mathbf{k},t)$ can be calculated as

$$\begin{aligned}\frac{\partial f_j(\mathbf{k},t)}{\partial k_x} &= \frac{\partial f_j(\mathbf{k}(\varepsilon),t)}{\partial \varepsilon}\frac{\partial \varepsilon_j(\mathbf{k})}{\partial k_x} \\ &= s_j \hbar v_{\mathrm{F}} \cos\theta_k \frac{\partial f_j(\mathbf{k}(\varepsilon),t)}{\partial \varepsilon},\end{aligned} \tag{3}$$

where $s_{j=1} = -1$ for valence band and $s_{j=2} = 1$ for conduction band. Then the distribution function can be analytically obtained as

$$\begin{aligned}f_j(\mathbf{k},\omega) = s_j \hbar v_{\mathrm{F}} \cos\theta_k \left(-\frac{qE(\omega)}{\hbar}\right) \\ \times \frac{\partial f_j^{(\mathrm{eq})}(\mathbf{k}(\varepsilon))}{\partial \varepsilon}\frac{1}{\left(-i\omega + \frac{1}{\tau_{\mathrm{scat}}}\right)}\end{aligned} \tag{4}$$

The x-directional current is then calculated as

$$\begin{aligned}J_x &= \frac{2_{\mathrm{valley}} 2_{\mathrm{spin}} q}{S}\sum_{j=\mathrm{C,V}} v_{\mathrm{F}} \sum_{\mathbf{k}} \cos\theta_k f_j(\mathbf{k}) \\ &= \sigma(\omega) E(\omega),\end{aligned} \tag{5}$$

where by replacing the summation over $\mathbf{k}$ by the integration we can finally obtain the conductivity

$$\sigma(\omega) = \frac{e^2}{\pi\hbar^2}\left[E_{\mathrm{F}} + 2k_{\mathrm{B}}T\log(1+e^{-\beta E_F})\right]\frac{1}{\left(-i\omega + \frac{1}{\tau_{\mathrm{scat}}}\right)}. \tag{5}$$

Taking the parameters used in [14] as an example, $T = 300$ K, $E_F = 0.5$ eV and $\tau_{\mathrm{scat}} = 1.0\times10^{-12}$ s, the corresponding conductivity values are shown in Fig. 5. The solid line shows the real value of graphene conductivity, whereas the dashed line shows the imaginary value. We can confirm that the real value dominates over imaginary value in the low frequency. Therefore, the imaginary value of conductivity can be ignored for simulations below 30 GHz (The maximum frequency of 5G wireless communication).

When modeling a graphene nanoantenna, we use the real value of graphene surface conductivity (in unit of [S]). In the 2-D simulation domain, a cross section of the antenna is taken in the xy plane. As shown in Fig. 6, the width of the antenna is assumed to be infinite in the $z-$ direction. The length L is in the $y-$ direction and the thickness t is in the $x-$ direction. The spatial mesh is $\Delta x = \Delta y = 2.5\times10^{-4}$ m. Using this mesh, a

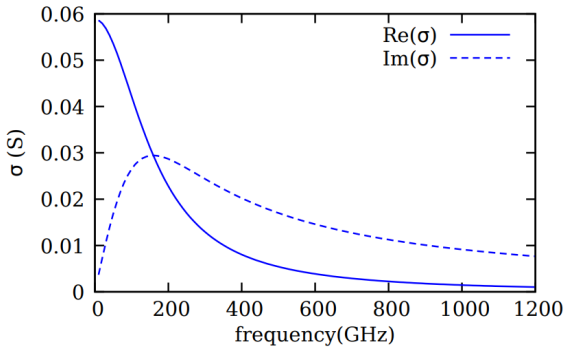

Fig. 5. The graphene surface conductivity (in unit of [S]) in frequency domain. We can see that the real value dominates over imaginary value in the low frequency.

$L = 5.0\times10^{-3}$ m graphene patch antenna is modeled by 20 cells along the $y-$ direction. The source excitation is a sine wave with a frequency of 30 GHz at the center of simulation domain, exciting a point wave with E_y polarization, incident onto the graphene antenna.

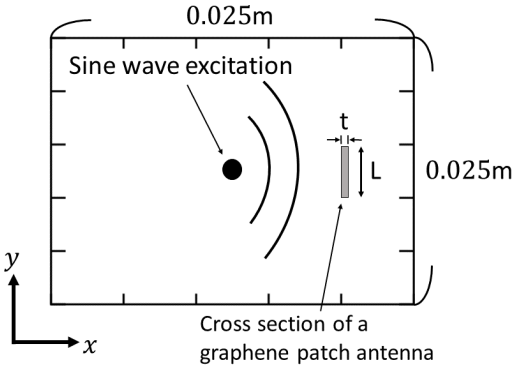

Fig. 6. The 2-D simulation domain is 0.025 m × 0.025 m square and has been discretized into 100 × 100 lattice points in the xy plane. Therefore, the spatial mesh is $\Delta x = \Delta y = 2.5\times10^{-4}$ m. Using this mesh, a $L = 5.0\times10^{-3}$ m graphene patch antenna is modeled by 20 cells along the $y-$ direction. The source excitation is a sine wave with a frequency of 30 GHz at the center of simulation domain, exciting a point wave with E_y polarization, incident onto the graphene antenna.

III. Results

In Fig 7, we show the temporal response of electric component E_y in time of $t = 25\Delta t, 50\Delta t, 75\Delta t, 100\Delta t$ respectively. As shown in these figures. The proposed simulation framework has been successfully worked and excited sine waves are propagated smoothly in the 2-D simulation domain. We can confirm that the graphene antenna is placed at $x = 0.020$ m and 0.010 m $\leq y \leq 0.015$ m, where the incident waves are reflected and diffracted.

In Fig 8, we show the temporal response of magnetic component H_z in time of $t = 25\Delta t, 50\Delta t, 75\Delta t, 100\Delta t$ respectively. We have excited a wave source only in E fields, but magnetic waves in H fields have been generated and propagated in the 2-D simulation domain. This is one of the typical characteristics of electromagnetic waves: varying the electric field gives rise to a time-varying magnetic field which in turn produces a time-varying electric field.

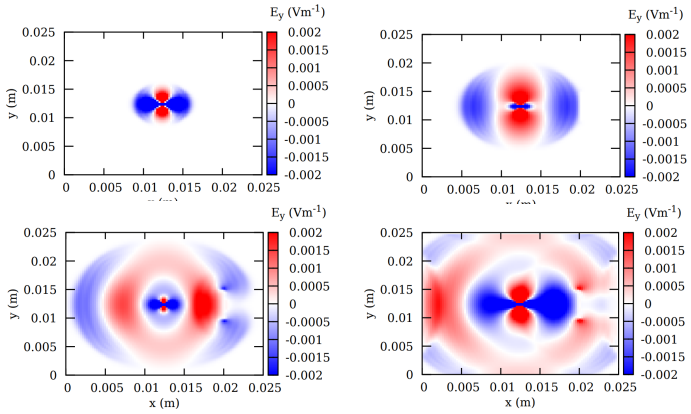

Fig. 7. The temporal response of electric component E_y in time of $t = 25\Delta t, 50\Delta t, 75\Delta t, 100\Delta t$ respectively. The source excitation is a point sine wave with a frequency of 30 GHz at the center of simulation domain, exciting a spherical wave with E_y polarization. We can see that the graphene antenna is placed at $x = 0.020$ m and 0.010 m $\leq y \leq 0.015$ m, where the incident waves are reflected and diffracted.

From the results of electric component E_y in Fig. 7, we have calculated the current density along the graphene antenna region ($x = 0.020$ m and 0.010 m $\leq y \leq 0.015$ m). In Fig. 9, We show the comparison of the current density (in unit of Am^{-1}) calculated from the real and imaginary conductivity of graphene given from Eq. (5) in time of $t = 25\Delta t, 50\Delta t, 75\Delta t, 100\Delta t$ respectively.

IV. Conclusion

We proposed a simulation framework of graphene nanoantenna based on Boltzmann equation and finite difference time-domain (FDTD) method. We have simulated transverse electric (TE) wave propagation and calculated the temporal response of electric component E_y and magnetic component H_z in time of $t = 0, 10\Delta t, 50\Delta t, 100\Delta t$ respectively. The proposed simulation framework has been successfully worked and the excited electromagnetic waves are propagated smoothly in the 2-D simulation domain. Also, we can confirm that the modeled graphene nanoantenna is functioned properly. On the surface of the antenna, the incident waves are reflected and diffracted.

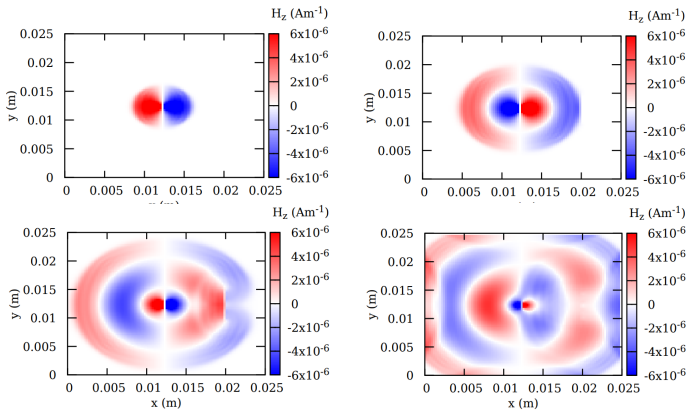

Fig. 8. The temporal response of magnetic component H_z in time of $t = 25\Delta t, 50\Delta t, 75\Delta t, 100\Delta t$ respectively. We have excited a wave source only in E fields, but magnetic waves in H fields have been generated and propagated in the 2-D simulation domain.

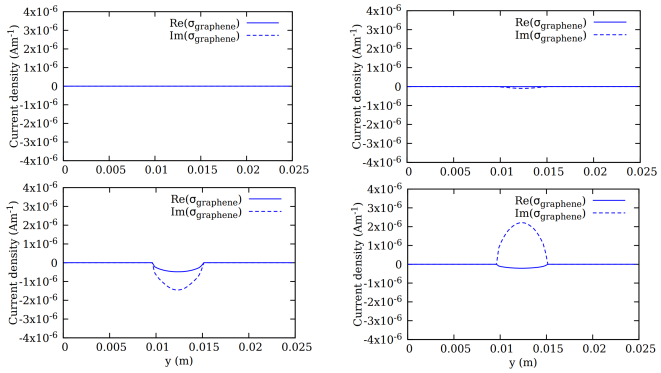

Fig. 9.

References

[1] K. S. Novoselov, A. K. Geim, S. V. Morozov, D. Jiang, Y. Zhang, S. V. Dubonos, I. V. Grigorieva, and A. A. Firsov, "Electric field in atomically thin carbon films," SCIENCE, **306**, 666 (2004). (DOI: 10.1126/science.1102896)

[2] A. K. Geim, K. S. Novoselov, "The rise of graphene," Nature Materials, **6**, 183 (2007). (DOI 10.1038/nmat1849)

[3] Y. Zhu, S. Murali, W. Cai, X. Li, J. W. Suk, J. R. Potts, and R. S. Ruoff, "Graphene and graphene oxide: Synthesis, properties, and applications," Adv. Mater, **22**, 3906 (2010).

[4] D. T. Nurrohman, N. F. Chiu, " A review of graphene-based surface plasmon resonance and surface-enhanced Raman scattering biosensors: Current status and future prospects," Nanomaterials, **11**, 216 (2021). (10.3390/nano11010216)

[5] M. A. AI Faruque, M. Syduzzaman, J. Sarkar, K. Bilisik, and M. Naebe, "A review on the production methods and applications of graphene-based materials," Nanomaterials, **11**, 2414 (2021). (DOI: 10.3390/nano11092414)

[6] T. Yusaf, A. S. F. Mahamude, K. Farhana, W. S. W. Harun, K. Kadirgama, D. Ramasamy, M. K. Kamarulzaman, S. Subramonian, S. Hall, and H. A. Dhahad, "A comprehensive review on graphene nanoparticles: Preparation, properties, and applications," Sustainability, **14**, 2336 (2022). (DOI: 10.3390/su141912336)

[7] A. Razaq, F. Bibi, X. Zheng, R. Papadakis, S. H. M. Jafri, and H. Li, "Review on graphene-, graphene oxide-, reduced graphene oxide-based flexible composites: From fabrication to applications," Materials, **15**, 1012 (2022). (DOI: 10.3390/ma15031012)

[8] S. K. Krishnan, N. Nataraj, M. Meyyappan, and U. Pal, "Graphene-Based Field-Effect Transistors in Biosensing and Neural Interfacing Applications: Recent Advances and Prospects," Analytical Chemistry, **95**, 2590. (2023) (DOI: 10.1021/acs.analchem.2c03399)

[9] A. Asadi, M. R. Jafari, and M. Shahmansouri, "Simulation optimized design of graphene-based hybrid plasmonic waveguide," Indian Journal of Physics, **97**, 2515 (2023). (DOI: 10.1007/s12648-023-02601-6)

[10] J. Miao, and T. Fan, "Flexible and stretchable transparent conductive graphene-based electrodes for emerging wearable electronics," Carbon, **202**, 495 (2023) (DOI: 10.1016/j.carbon.2022.11.018)

[11] N. Kiani, F. T. Hamedani, and P. Rezaei, "Designing of a circularly polarized reconfigurable graphene-based THz patch antenna with cross-shaped slot," Optical and Quantum Electronics, **55** (2023). (DOI: 10.1007/s11082-023-04617-y)

[12] K. Yee, "Numerical solution of initial boundary value problems involving maxwell's equations in isotropic media," IEEE Transactions on Antennas and Propagation, **14**, 302 (1966). (DOI: 10.1109/TAP.1966.1138693)

[13] J. Du, B. Tong, S. Yuan, N. Dai, R. Liu, D. Zhang, H. Cheng, and W. Ren, "Advances in Flexible Optoelectronics Based on Chemical Vapor Deposition-Grown Graphene," Advanced Functional Materials, **32** (2022). (DOI: 10.1002/adfm.202203115)

[14] X. Yu, "FDTD Modeling of Graphene-Based RF Devices: Fundamental Aspects and Applications," M. S. thesis, University of Toronto (2013).